Genetic Ablation of PKC Epsilon Inhibits Prostate Cancer Development and Metastasis in Transgenic Mouse Model of Prostate Adenocarcinoma

Bilal Bin Hafeez[1], Weixiong Zhong[2], Jamey Weichert[3], Nancy E. Dreckschmidt[1], Mohammad Sarwar Jamal[1], and Ajit K. Verma[1]

Abstract

Protein kinase C epsilon (PKCε), a novel PKC isoform, is overexpressed in prostate cancer (PCa) and correlates with disease aggressiveness. However, the functional contribution of PKCε to development or progression of PCa remained to be determined. Here we present the first *in vivo* genetic evidence that PKCε is essential for both the development and metastasis of PCa in the transgenic mouse model of prostate adenocarcinoma (TRAMP). Heterozygous or homozygous genetic deletions of PKCε in FVB/N TRAMP inhibited PCa development and metastasis as analyzed by positron emission tomography/computed tomography, tumor weight determinations, and histopathology. We also examined biomarkers associated with tumor progression in this model, including markers of survival, proliferation, angiogenesis, inflammation, and metastatic progression. To find clues about the genes regulated by PKCε and linked to the Stat3 signaling pathway, we carried out focused PCR arrays of JAK/STAT signaling in excised PCa tissues from PKCε wild-type and nullizygous TRAMP mice. Notably, PKCε loss was associated with significant downregulation of proliferative and metastatic genes *C/EBPβ* (CCAAT/enhancer binding protein β), *CRP* (C-reactive protein), *CMK*, *EGFR* (epidermal growth factor receptor), *CD64*, *Jun B*, and *gp130*. Taken together, our findings offer the first genetic evidence of the role of PKCε in PCa development and metastasis. PKCε may be potential target for prevention and/or treatment of PCa. *Cancer Res; 71(6); 2318–27.* ©*2011 AACR.*

Introduction

Prostate cancer (PCa) is the most common type of cancer in American men and ranks second to lung cancer in cancer-related deaths. The American Cancer Society has estimated that 217,730 new cases will be diagnosed and 32,050 deaths will occur in the United States alone in the year of 2010 (1). The lack of effective therapies for advanced PCa is related to a large extent to the poor understanding for the molecular mechanisms underlying the progression of the disease toward invasion and metastasis (2). Therefore, defining the novel molecular targets linked to PCa progression and metastasis will improve the planning strategies for the prevention and treatment of PCa.

Authors' Affiliations: [1]Department of Human Oncology, Wisconsin Institute of Medical Research, Paul Carbone Comprehensive Cancer Center, School of Medicine and Public Health; [2]Department of Pathology and Laboratory Medicine, University of Wisconsin, and William S. Middleton Memorial Veterans Hospital; and [3]Department of Radiology, School of Medicine and Public Health, University of Wisconsin, Madison, Wisconsin

Corresponding Author: Ajit K. Verma, Department of Human Oncology, School of Medicine and Public Health, University of Wisconsin, Madison, WI 53792. Phone: 608-263-8526; Fax: 608-262-6654; E-mail: akverma@facstaff.wisc.edu

doi: 10.1158/0008-5472.CAN-10-4170

PKC is a major intracellular receptor for the mouse skin tumor promoter 12-*O*-tetradecanoylphorbol-13-acetate. It represents a large family of phosphatidylserine (PS)-dependent serine/threonine kinases (3–7). On the basis of structural similarities and cofactor dependence, 11 PKC isoforms have been classified into 3 subfamilies: the classic (cPKC), the novel (nPKC), and the atypical (aPKC). The cPKCs (α, βI, βII, γ) are dependent on PS, diacylglycerol (DAG), and Ca^{2+}. The nPKCs (δ, ε, η, and) retain responsiveness to DAG and PS but do not require Ca^{2+} for full activation. The aPKCs (λ and ζ) require only PS for their activation (3–5). PKC epsilon (PKCε) is involved in the regulation of diverse cellular functions including gene expression, neoplastic transformation, cell adhesion, mitogenicity, and cell invasion (8, 9).

PKCε has been considered to be the hallmark of PCa development. Evidence suggests that overexpression of PKCε is sufficient to promote conversion of androgen-dependent LNCaP cells to androgen-independent (AI) variant, which rapidly initiates tumor growth *in vivo* in both intact and castrated athymic nude mice (10). A recent study has shown that overexpression of PKCε protected LNCaP cells against apoptotic stimuli via inducing phosphorylation of Bad at Ser112 residue (11). It has been shown that integrin signaling links PKCε to the PKB/AKT survival pathway in recurrent PCa cells (12). Proteomic analysis of PCa CWR22 cells xenografts show that association of PKCε with Bax may

neutralize apoptotic signals propagated through the mitochondrial death signaling pathway (13). We and others have previously shown that PKCε level correlates with the aggressiveness of human PCa. Also, PKCε is overexpressed in PCa spontaneously developed in transgenic adenocarcinoma of the mouse prostate (TRAMP) mice, an autochthonous transgenic model that mimics to the human disease (14). We have also shown that PKCε is a protein partner of transcription factor Stat3. PKCε associates with Stat3 and this association increases with the progression of the diseases in TRAMP mice and in human PCa. Taken together, all these findings suggest that *PKC*ε is an oncogene and is involved in PCa development and aggressiveness and in the emergence of AI PCa (14). However, the role of PKCε in PCa development and progression in intact mouse model remains elusive. We present here for the first time that genetic loss of PKCε in TRAMP mice prevents development and metastasis of PCa, possibly via downregulation of proliferative and metastatic genes.

Materials and Methods

Antibodies

Monoclonal or polyclonal antibodies specific for Bcl-xL, β-actin, COX-2, gp130, GAPDH (glyceraldehyde 3-phosphate dehydrogenase), PKCε, PKCα, PKCδ, PKCβII, PKC, PKCγ, PKCλ, PKCζ PKCε, PI3K85, PI3K110, PCNA (proliferating cell nuclear antigen), total Stat3, total Stat5, and VEGF were purchased from Santa Cruz Biotechnology. Blocking peptides for gp130 and Stat3 antibodies and mouse IgG were also procured from Santa Cruz Biotechnology. Monoclonal antibodies specific for pStat3Tyr705, and pStat3Ser727 were obtained from BD Biosciences. Antibodies specific to pAKTSer308, pAKTSer473, and total AKT were purchased from Cell Signaling Technology.

Experimental animals

FVB-TRAMP mice were provided by Dr. Barbara Foster, Roswell Park Cancer Institute, Buffalo, NY. PKCε KO mice were generated and provided by Dr. Michael Leitges, Max-Plank-Institut Fur Immunoliologie, and Freiburg, Germany. To create the bigenic mice, TRAMP mice (TG/WT//+/+) were crossbred with heterozygous (Het) null PKCε (WT/WT//−/+). TG/WT//−/+ and WT/WT//−/+ mice were obtained and crossbred to generate the TRAMP-PKCε WT (WT), TRAMP-PKCε Het (Het), and TG//PKCε KO (KO) mice. A total of 21 mice containing TG ($n = 7$), Het ($n = 7$), and KO ($n = 7$) were used for the study. After 18 weeks, all the mice of TG, Het, and KO groups were euthanized and their blood was collected for serum preparation.

PET/CT scanning

Two animals from each group (TG, Het, and KO) were used for positron emission tomography (PET)/computed tomography (CT). We utilize a radioiodinated phospholipid ether analogue, ^{124}I-NM404. Following injection with ^{124}I-NM404, animals were anesthetized with isoflurane and scanned at desired time intervals by hybrid micro-CT/PET (100-μm spatial CT resolution, 40 million PET counts, filtered back projection image reconstruction).

Histopathologic examination

Prostate, lung, kidney, liver, and lymph nodes were excised and processed for histology as described previously (15).

IL-6 ELISA assay

Interleukin 6 (IL-6) levels were determined from mouse serum by using specific ELISA kit for mouse IL-6 (eBioscience, Inc.). All of the procedures were followed by the manufacturer's protocol.

Immunoblot analysis

Tissues from PCa and brain were excised and whole tissue lysates were prepared. In brief, part of the PCa and brain tissues of TG, Het, and KO mice were homogenized in lysis buffer [50 mmol/L HEPES, 150 mmol/L NaCl, 10% glycerol, 1% Triton X-100, 1.5 mmol/L $MgCl_2$, 10 μg/mL aprotinin, 10 μg/mL leupeptin, 1 mmol/L phenylmethylsulfonyl fluoride (PMSF), 200 μmol/L Na_3VO_4, 200 μmol/L NaF, and 1 mmol/L EGTA (final pH 7.5)]. The homogenate was centrifuged at 14,000 × *g* for 30 minutes at 4°C. Supernatants were collected and stored at −80°C until further use. Protein was estimated using Bio-Rad protein assay kit as per the manufacturer's protocol. Forty micrograms of tissue lysate were fractionated on 10% criterion precast SDS-polyacrylamide gel (Bio-Rad Laboratories). The protein was transferred to 0.45 μm Hybond-P polyvinylidene difluoride transfer membrane (Amersham Life Sciences). The membrane was then incubated with the indicated antibody followed by a horseradish peroxidase secondary antibody (Thermo Scientific), and the detection signal was developed with Amersham's enhanced chemiluminescence reagent using FOTO/Analyst Luminary Work Station (Fotodyne Inc.). The Western blots were quantitated by densitometric analysis by using Totallab Nonlinear Dynamic Image analysis software (Nonlinear USA, Inc.).

Electrophoretic mobility shift assay

Nuclear extracts were prepared from prostate tissues from TG, Het, and KO mice in a high-salt buffer [20 mmol/L HEPES (pH 7.9), 20 mmol/L NaF, 1 mmol/L $Na_3P_2O_7$, 1 mmol/L Na_3VO_4, 1 mmol/L EDTA, 1 mmol/L EGTA, 1 mmol/L DTT, 0.5 mmol/L PMSF, 420 mmol/L NaCl, 20% glycerol, 1 μg/mL leupeptin, and 1 μg/mL aprotinin]. The samples were then centrifuged and harvested. Protein was estimated by using protein assay kit (Bio-Rad) as per the manufacturer's protocol. Stat3 DNA binding activity was determined in individual mouse nuclear lysates of each group. In brief, nuclear extracts (10 μg) were incubated in a final volume of 20 μL of 10 mmol/L HEPES (pH 7.9), 80 mmol/L NaCl, 10% glycerol, 1 mmol/L DTT, 1 mmol/L EDTA, and 100 μg/mL poly (deoxyinosinic-deoxycytidylic acid) for 15 minutes. A P^{32}-radiolabeled double-stranded Stat3 consensus binding motif 5′-GATCCTTCTGGGAATTCCTAGATC-3′ (Santa Cruz Biotechnology) probe was then added and incubated for 20 minutes at room temperature. The protein–DNA complexes were resolved on a 4.5% nondenaturing polyacrylamide gel containing 2.5% glycerol in

0.25× Tris-borate EDTA at room temperature, and gels were dried and autoradiographed. Stat3 DNA binding activities were determined.

Immunohistochemistry

To determine the expression of Stat3, IL-6 receptor (IL-6R), and PCNA proteins in prostatic intraepithelial neoplasia (PIN) and moderately and poorly differentiated (PD) adenocarcinoma of each mouse of TG and KO, we conducted immunohistochemistry in paraffin-embedded sections (4-μm thickness). In brief, sections were deparafffinized by placing the slides at 60°C for 2 hours followed by 3 changes of xylenes for 10 minutes each. Slides were placed in 0.3% methanol/hydrogen peroxide for 20 minutes for quenching endogenous peroxidase. Slides were rehydrated in one change of absolute, 95%, 75%, and 50% ethanol and distilled water. Antigen retrieval was carried out by incubating samples at 116°C for 15 seconds in the declocking chamber by using a Tris–urea solution (pH 9.5). After antigen retrieval, tissues slides were incubated with 2.5% normal horse serum (R.T.U. Vectastain Universal Elite ABC Kit; Vector Laboratories) for 20 minutes to block nonspecific binding of the antibodies. Subsequently, the slides were incubated over night with a mixture of Stat3 (1:50), IL-6R (1:50), and PCNA (1:50) dilution in normal antibody diluents (Scy Tek # ABB-125) in a humidified chamber. Blocking peptides of Stat3 and IL-6 antibodies were used to determine the specific immunoreactivity of these antibodies. We further confirmed the specificity of immunostaining of PCNA, IL-6, and Stat3 by using IgG antibody (served as a negative control). The mixture of antibodies was decanted, and the slides were washed thrice in TBS (pH 7.4). The slides were incubated with appropriate secondary antibodies for 30 minutes at room temperature. Slides were rinsed with TBS for 5 minutes and ABC reagent (Vector kit) was applied for 30 minutes. Immunoreactive complexes were detected using 3,3′-diaminobenzidine substrate (Thermo Scientific) and counter stained by using hematoxylin (Fischer Scientific) for nuclear staining. Finally, slides were mounted with cover slip by using mounting medium. All sections were visualized under a Zeiss-Axiophot DM HT microscope and images were captured with an attached camera. Dr. Weixiong Zhong, MD, a certified pathologist, examined all the slides. For the quantification of Stat3- and PCNA-positive staining cells, 5 random areas were selected from each slide of TG and KO mice. The number of cells showing positive labeling and the total number of cells counted were recorded. An average percentage was then calculated on the basis of the total number of positive staining cells from each set of 5 fields counted. Results are expressed as mean ± SEM.

Quantitative real-time PCR array

Changes in expression of genes involved in the JAK/STAT signaling pathway was determined using real-time PCR (RT-PCR) arrays. In brief, excised PCa tissue from TG and KO mice were snap frozen and stored at −80°C. Total RNA was isolated using TRIzol reagent (Invitrogen) as per the manufacturer's instruction. RNA concentration and purity were checked by UV spectrophotometry, and RNA integrity was determined by electrophoresis. The first cDNA strand was synthesized using RT^2 First Strand Kit (SA Biosciences). The cDNA from either TG or KO PCa tissues was then applied to the RT^2 Profiler PCR Array for the JAK/STAT pathway (SA Biosciences) according to manufacturer's instructions. The RT-PCR reactions were run on the MyIQ (Bio-Rad) and the results (C_t), normalized to β-actin (ΔC_t), were determined using iQ5 software (Bio-Rad). Fold expression was determined as, where $\Delta\Delta C_t$ is $\Delta C_{t(KO)} - \Delta C_{t(TG)}$.

Statistical analysis

Student's t test was carried out to determine the significance. $P < 0.05$ was considered as significant.

Results

Generation and characterization of PKCε-deleted TRAMP mice

As shown in Figure 1A, TG, Het, and KO mice were generated by cross-breeding 6 to 7 weeks old homozygous TRAMP with PKCε Het mice (Fig. 1A). Both TRAMP and PKCε KO mice were on FVB/N background. No PKCε expression was observed in either prostate or brain excised tissues of KO mice [Fig. 1B and C (i and ii)]. A significant decrease in protein levels of PKCε was observed in the prostate of Het mice compared with TG mice (Fig. 1B). To determine whether deletion of PKCε has any compensatory effect in TRAMP mice, we carried out immunoblot analysis of PKC isoforms in prostate and brain tissue lysates of TG, Het, and KO mice. Results indicate no change in the expression of other PKC isoforms in brain tissue of Het and KO mice [Fig. 1C (i and ii)], suggesting no compensatory effects in PKCε-deleted TRAMP mice.

Deletion of PKCε in TRAMP mice inhibits PCa development and metastasis

Accumulating evidence now indicates that *PKCε* is an oncogene which plays a vital role in the development of various types of human cancers including the prostate. Molecular genetic evidence of the role of PKCε in PCa development in an intact mouse model still remains obscure. In this study, we explored the possibility whether PKCε deletion in TRAMP mice inhibits the development and metastasis of PCa. A total of 21 mice (TG, $n = 7$; Het, $n = 7$; and KO, $n = 7$) were used in this study. In our first experiment, we carried out micro-PET/CT imaging, using a tumor selective radiopharmaceutical agent ^{124}I-NM404 (16), of two 16 weeks old mice from each of TG and KO mice [Fig. 2A (i) and B (i)]. Results illustrated a lack of focal uptake of ^{124}I-NM404 in KO mice [Fig 2B (i and ii)] compared with TG mice [Fig. 2A (i and ii)]. TG mice showed metastasis in proximal lymph node as evident by uptake of ^{124}I-NM404 [Fig. 2A (i and ii)]. However, no metastasis was observed in KO mice, suggesting the role of PKCε in the development and metastasis of PCa. All of the remaining mice from each group were sacrificed at the same age (18 weeks). Their bloods were collected from retro-orbital plexus for serum isolation. PCa tissues were excised and parts of the tissues were used in preparation of whole tissue lysates, nuclear lysates, RNA isolation, and histology sectioning as

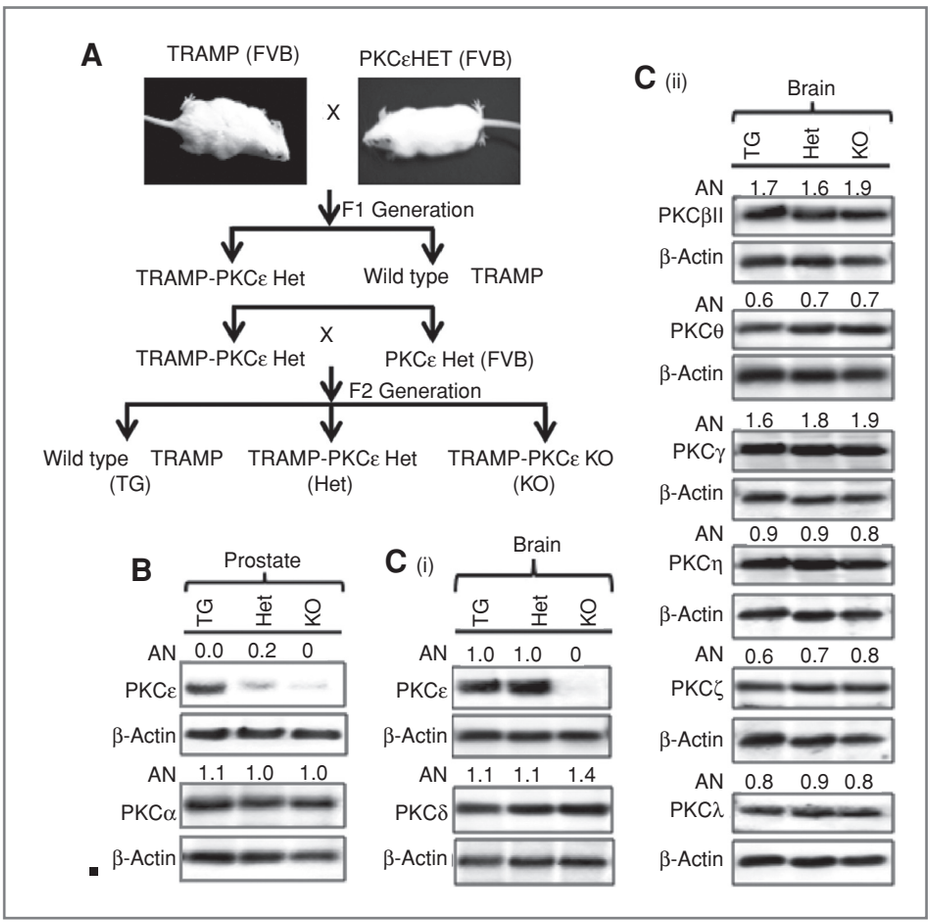

Figure 1. Generation and characterization of PKCε-deleted TRAMP mice. A, scheme for generation of bigenic PKCε KO TRAMP mice. Both TRAMP and PKCε KO mice were on FVB/N background. TG, Het, and KO mice were evaluated for the development of PCa. B and C, Western blot analysis of PKC expression in PCa and brain tissues lysates (40 μg protein) from 18 weeks old TG, Het, and KO mice. Protein levels of PKCε and PKCα in PCa tissues (B) and PKC isoforms in brain tissues (C, iii). Equal loading of protein was determined by stripping and reprobing the blots with β-actin antibody. Values in arbitrary number (AN) shown above the immunoblots represent densitometer quantitation of band normalized to β-actin.

described in Material and Methods. Parts of the tissues excised from the kidneys, brains, livers, lungs, and lymph nodes were fixed in 10% buffered formalin and used for histopathology. Deletion of PKCε in TRAMP mice, or even one allele deletion, shows significant ($P < 0.01$) reduction in growth of PCa in all of the Het and KO mice (Fig. 2C and D). All TG mice developed 1 or 2 large-sized prostate tumors (Fig. 2C), whereas Het and KO mice had only a single small-sized tumor (Fig. 2C). One of the TG mice also showed grossly visible metastases in a local lymph node, both lungs, and the left kidney, which were confirmed by light microscopy (Fig. 2E and F). In addition, microscopic metastases were identified in another 3 TG mice. No metastasis was identified in any of the Het and KO mice (Fig. 2G and H). Hematoxylin and eosin (H&E)-stained tissue sections showed that all the grossly visible tumors were PD carcinomas characterized by solid sheets of large polymorphic cancer cells, with a high nucleus-to-cytoplasm ratio, frequent apoptosis, central necrosis, and neuroendocrine differentiation [Fig. 3D (i) and E (i)]. Some of the Het and KO mice showed small foci of PD carcinoma at the microscopic level only. In addition, all the mice showed PIN characterized by epithelial cell proliferation with enlarged hyperchromatic nuclei and nuclear stratification in papillary and cribriform structures [Fig. 3D (i) and E (i)].

Deletion of PKCε in TRAMP mice inhibits Stat3 activation

Aberrant activation of Stat3 has been linked to the progression of PCa metastasis (17–19). A study suggests that overexpression of Stat3 in normal prostate epithelial cells leads to conversion of malignant phenotype (20). To determine whether PKCε deletion in TRAMP mice inhibits Stat3 activation, we carried out immunoblot analysis in excised tissue PCa lysates of TG, Het, and KO mice. Results illustrated significant inhibition of both Ser727 and Tyr705 phosphorylation of Stat3 in both Het and KO mice (Fig. 3A). A significant decrease in DNA binding activity of Stat3 was observed in Het and KO mice [Fig. 3B (i and ii)]. Immunohistochemistry results show a significant decrease in intensity of nuclear staining of Stat3 in PIN and PD PCa of KO mice [Fig. 3C and E (ii)] compared with those in TG mice [Fig. 3D (ii)]. Specificity of Stat3 staining in TG PCa tumor tissue was confirmed using blocking peptide of Stat3 (Fig. 3F).

Deletion of PKCε inhibits serum IL-6 and IL-6R gp130 expression

We have previously shown elevated levels of IL-6 in TRAMP mice compared with nontransgenic mice at the same age (14). To determine whether deletion of PKCε in TRAMP mice decreases serum IL-6 levels, we carried out specific ELISA

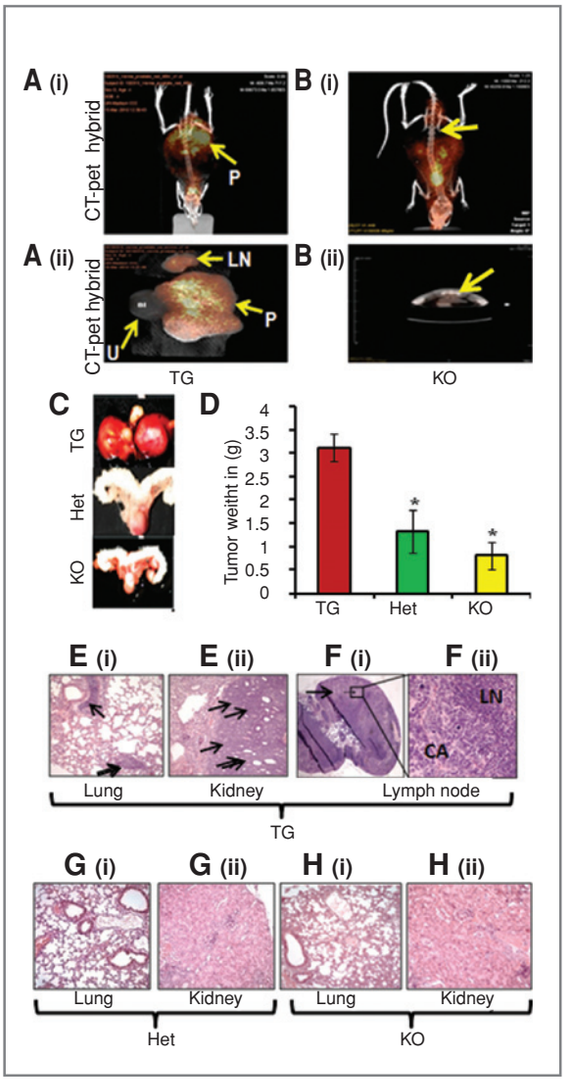

Figure 2. Deletion of PKCε in TRAMP mice inhibits development and metastasis of PCa. TG ($N = 7$), Het ($N = 7$), and KO ($N = 7$) male mice were evaluated for the development of PCa. Hybrid micro-PET/CT image acquired 48 hours post–^{124}I-INM404 intravenous injection to TG (A) and KO (B) mice at 18 weeks. Hybrid micro-PET/CT images of excised prostate tumor of TG (A, i-ii) and KO mice (B, i-ii). U, LN, and P denote urinary bladder, proximal lymph node, and PCa, respectively. Arrow denotes prostate in B, i-ii. C, representative photographs of excised urogenital tracts of TG, Het, and KO mice at 18 weeks. D, bar graph illustrates excised prostate tumor weight of TG, Het, and KO mice. Each value in the bar graph represents mean ± SEM of 5 different mice. Student's t test was carried out to evaluate the significant difference ($P < 0.01$). Representative photographs of H&E staining of lung (E, i), kidney (E, ii), and lymph node (F, i and ii). Enlarged image of lymph node (F, i) showing normal lymphocytes and PCa metastases (F, ii). Arrows indicate metastases of PCa in the lung, kidney, and lymph node of TG mice. Representative photographs of H&E-stained tissue sections of lung (G, i) and kidney (G, ii) of Het mice and lung (H, i) and kidney (H, ii) of KO mice.

for mouse IL-6 and observed a significant ($P < 0.05$) decrease in serum IL-6 levels in Het and KO mice compared with TG mice (Fig. 4H), suggesting that PKCε might be initiator of the IL-6/Stat3 signaling pathway. *IL-6R* (*gp130*) is one of the downstream target genes of Stat3. Immunohistochemistry results showed a significant decrease in the protein levels of IL-6R in KO mice compared with TG mice (Fig. 4A). Weak immunostaining of IL-6R was observed in benign epithelial cells and moderate staining in PD carcinoma cells of both TG and KO mice [Fig. 4E (i)], although there is strong immunostaining of IL-6R in PIN of TG mice and only moderate staining in PIN of KO mice [Fig. 4D (i)]. Specific immunoreactivity of IL-6R was confirmed by using blocking peptide of IL-6R antibody [Fig. 4F (i)].

Deletion of PKCε inhibits markers of proliferation, antiapoptosis, and metastasis

Evidence from published studies, including our laboratory, suggests modulation of various apoptotic and proliferative biomarkers in PCa in both humans and TRAMP mice during the progression and metastasis (14, 21). To determine possible changes in biomarkers involved in apoptosis, proliferation, and metastasis of PCa in PKCε-deleted TRAMP mice, we conducted immunoblot analysis of selected biomarkers in PCa tissue lysates of TG, Het, and KO mice. We observed a decrease in the protein levels of Bcl-xL, COX-2, cyclin D1, and VEGF in Het and KO mice (Fig. 4A and B). We have previously shown overexpression of PI3K/AKT in PCa tissues of TRAMP mice compared with nontransgenic prostate tissues at the same age (14). We observed a decrease in the protein levels of regulatory subunit (p85β) of PI3K in Het and KO mice but no change was observed in the protein levels of catalytic isoform (p110β) of PI3K (Fig. 4B), pAKTSer473, or pAKTSer308 (Fig. 4C). We also carried out immunohistochemistry of PCNA in PCa tissues of TG and KO mice and observed a significant decrease in the nuclear levels of PCNA in PIN and PD PCa of KO mice [Fig. 4E (ii)–G].

Quantitative PCR array identifies decreased transcripts of genes implicated in PCa development and metastasis

To further define the role of PKCε in modulating the other genes associated with JAK/STAT3 signaling and involved in PCa development and metastasis, we carried out quantitative RT-PCR (qRT-PCR) array of genes associated with JAK/STAT signaling pathway on total RNA isolated from PCa tissues of TG and KO mice. This array contained 84 genes related to JAK/STAT family members, the receptors that activate them, nuclear cofactor and coactivators associated with the Stat proteins, Stat-inducible genes, and negative regulators. A significant decrease in the mRNA expression of CCAAT/enhancer binding protein β (*C/EBPβ*; 2.5-fold), C-reactive protein (*CRP*; 4.34-fold), epidermal growth factor receptor (*EGFR*; 4.54-fold), *gp130* (2.5-fold), *Jun B* (2.5-fold), and *Stat3* (2.85-fold) was observed in KO mice compared with TG mice (Table 1). These results indicate that PKCε directly and/or indirectly regulates the expression of *Stat3* and Stat3 downstream target genes involved in PCa development and metastasis.

Discussion

In this study, we for the first time investigated PKCε link between the development and metastasis of PCa in transgenic

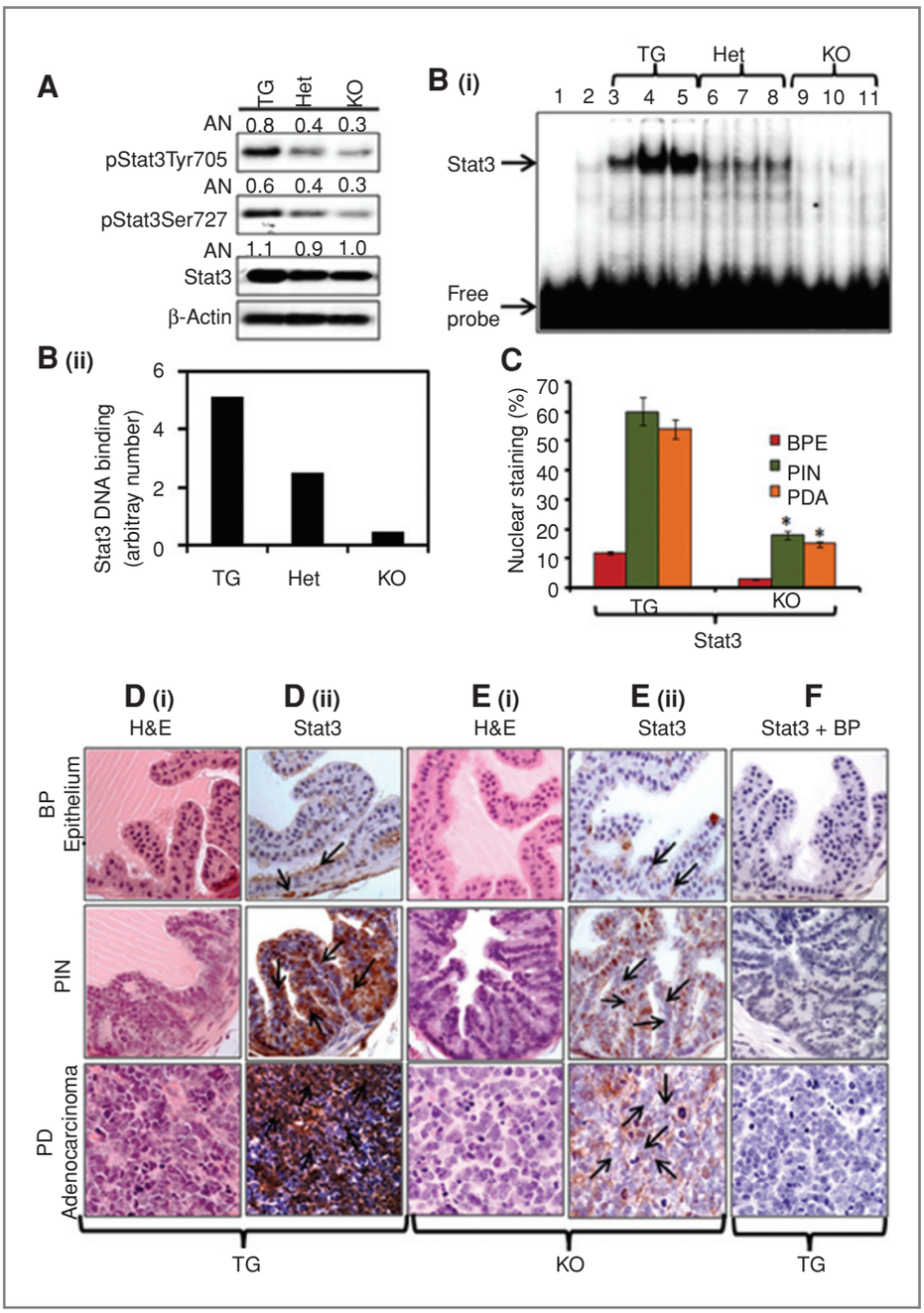

Figure 3. Deletion of PKCε in TRAMP mice inhibits Stat3 activation. PCa tissues from TG, Het, and KO mice were excised and whole cell lysates were prepared and used for Western blot analysis as described in Materials and Methods. A, protein levels of pStat3Tyr705, pStat3Ser727, and total Stat3. Equal loading of protein was determined by stripping and reprobing the blots with β-actin antibody. Values in AN shown above the immunoblots represent quantitation of the bands normalized to β-actin as described in Materials and Methods. B, i, DNA binding activity of Stat3 in PCa tissues of TG, Het, and KO mice as determined by EMSA. Lane 1 is free probe. Specificity of Stat3 DNA binding was determined by mutant probe of Stat3 (lane 2). B, ii, quantitative analysis of EMSA of Stat3 DNA binding activity of TG, Het, and KO mice. C, bar graph represents quantification of Stat3 nuclear staining of TG and KO prostate tumor tissues. Student's *t* test was carried out to analyze nuclear staining difference ($P < 0.05$). D, i through E, ii, representative photographs of (H&E) staining and immunohistochemistry of Stat3 in benign prostate (BP) epithelium, PIN, and PD adenocarcinoma of TG and KO mice. Arrows indicate the nuclear staining of Stat3. F, specificity of Stat3 antibody by using Stat3 blocking peptide.

mouse model (TRAMP). We used a molecular genetic approach to generate bigenic TRAMP mice, which were also either wild-type, heterozygous null, or homozygous null for PKCε. Deletion of PKCε did not affect other isoforms of PKC in Het or KO mice, suggesting no compensatory effect of PKCε deletion in TRAMP mice. All of the PKCε-deleted TRAMP mice were healthy and we did not observe any gross pathologic changes in any organs of these animals.

TRAMP PCa closely mimics human PCa, as they both spontaneously develop progressive PCa. TRAMP PCa is invasive and capable of metastasis to distant sites, primarily to pelvic lymph nodes and to the lungs (22). Mouse genetic background affects the development of TRAMP PCa. TRAMP mice on FVB/N background more readily develop PIN compared with TRAMP mice on C57Black/B16 background (22). In our study, we observed that deletion of PKCε in TRAMP mice prevents tumor development, which was evident by a lack of focal uptake of ^{124}I-NM404, a selective tumor agent [Fig. 2B (ii)]. This was followed by a significant ($P < 0.01$) decrease in prostate tumor weight in Het and KO animals (Fig. 2C and D).

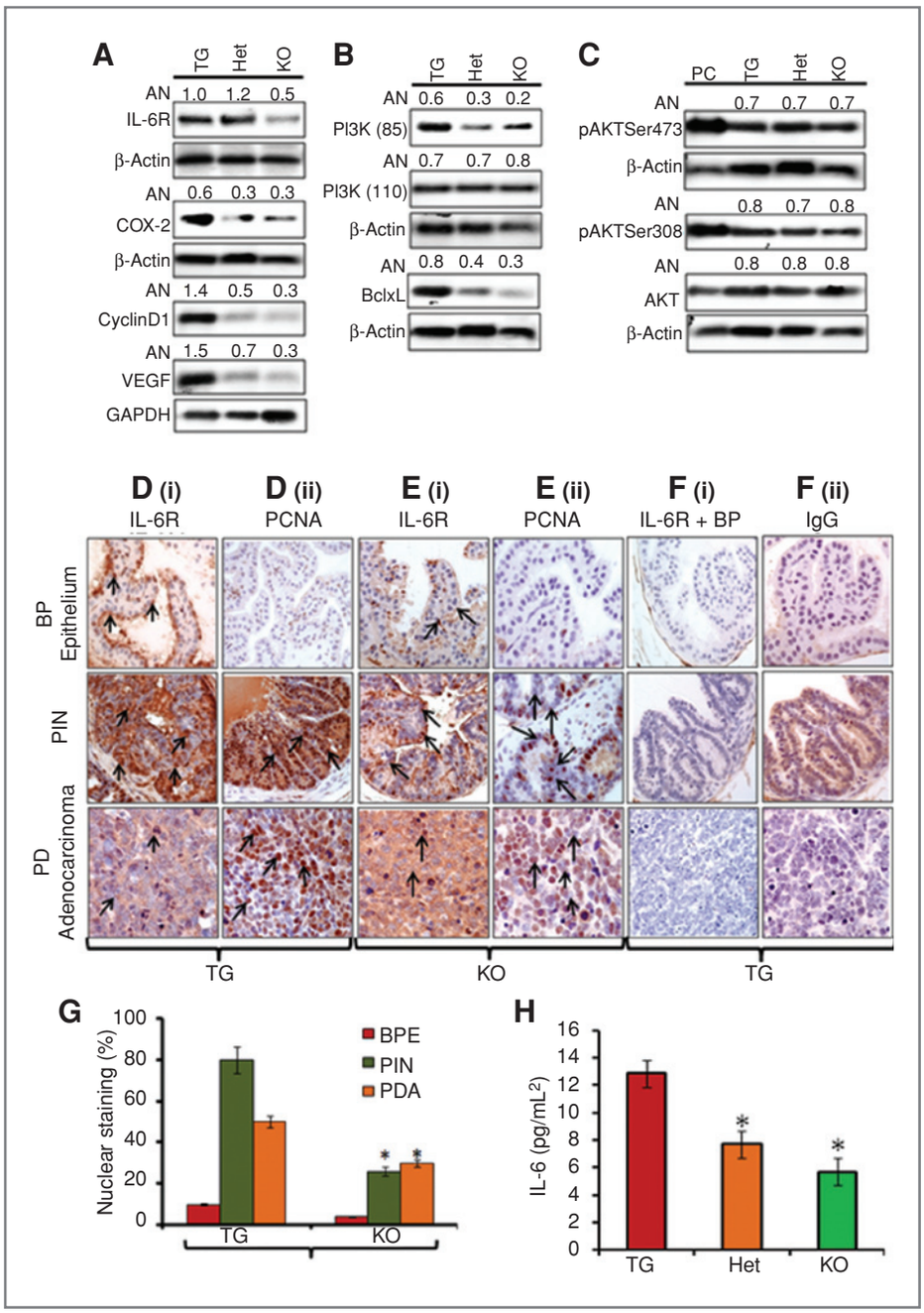

Figure 4. Deletion of PKCε in TRAMP mice inhibits expression of antiapoptotic and proliferative markers and decreases serum IL-6 level. PCa tissues of 18 weeks old TG, Het, and KO mice were excised and homogenized in the lysis buffer for Western blot analysis as described in Materials and Methods. Proteins (40 μg) were subjected on 10% to 15% Tris-HCl SDS-PAGE and immunoblotted using appropriate antibodies. Equal loading of protein was determined by stripping and reprobing the blots with β-actin or GAPDH antibodies. Values in AN above the immunoblots represent quantitation of the bands normalized to β-actin or GAPDH as described in Materials and Methods. A, expression level of IL-6R, COX-2, cyclin D1, and VEGF. B, expression of PI3K (85), PI3K (110), and Bcl-xL. C, expression level of pAKTSer473, pAKTSer308, and total AKT. D and E, representative photographs of immunohistochemistry of IL-6R and PCNA in benign prostate (BP) epithelium, PIN, and PD adenocarcinoma of TG (D, i and ii) and KO (E, i and ii) mice. Arrows indicate immunoperoxidase labeling of IL-6 and PCNA. F, i, specificity of IL-6 antibody by using IL-6 blocking peptide. F, ii, negative control by using IgG. G, bar graph represents quantification of PCNA nuclear staining in BP, PIN, and PD of TG and KO mice. Student's *t* test was carried out to analyze nuclear staining difference ($P < 0.05$). H, serum IL-6 levels as determined by ELISA kit for mouse IL-6. Each value in the bar graph represents the mean ± SEM of IL-6 level from 3 mice. Results indicate a significant decrease ($P < 0.05$) in the levels of serum IL-6 in Het and KO mice compared with TG mice.

Metastasis of PCa to distant organs is the main cause of morbidity and mortality in PCa patients. Importantly, we observed the metastasis of PCa to lungs, lymph nodes, and kidneys of the 70% TG animals, which was evident by the uptake of ^{124}I-NM404 into the lymph nodes. Histopathologic examinations of lungs, lymph nodes, and kidneys of TG mice further confirm the metastasis of PCa. However, no metastasis was detected in any of the animals, even in the 2 mice from each Het and KO groups that had PCa. Taken together, these results strongly support that loss of PKCε inhibits both primary PCa and metastasis.

PCa is heterogeneous in nature, which involves activation of multiple signaling pathways. Constitutive activation of the transcription factor Stat3 has been shown to be a marker of poor prognosis in human PCa. Activation of Stat3 has been linked to the PCa development and metastasis through the induction of various genes responsible for tumor cell proliferation, cell survival, and carcinogenesis (17–19). In our previous studies, we have shown that PKCε activates and physically interacts with Stat3 in various types of human cancer cells including the prostate (23). In this study, loss of PKCε in TRAMP mice inhibited activation of Stat3, which

Table 1. List of genes that significantly modulated in KO mice compared with TG mice

Name of the gene	Symbol	Fold decrease/ increase	Biological function
No. of genes downregulated in KO mice compared with TG mice			
CRP2	Cebpb	2.5	Cell proliferation and inflammation, upregulates metastatic genes
Al255847	Crp	4.34	Serum biomarker in various cancers, prognostic marker in castrated-resistant PCa
CMK	CxCL9	2.94	T-cell trafficking
ERBB	EGFR	4.54	Member of Erbb2 family, cell proliferation, angiogenesis, invasion, metastasis, and inhibition of apoptosis, involved in angiogenesis and metastasis of PCa
Epor	Epor	3.57	Glycoprotein hormone, belongs to serine/threonine and tyrosine family regulators of red blood cells in mammals, overexpressed in PCa tissues
CD64	Fcgr1	2.56	Stimulates cell proliferation of macrophages, develops resistance to chemotherapeutic drugs, and radiation therapy
UCRP	Isg15	3.0	Interferon-regulated protein involved in cell growth, cell cycle
GHR	Ghr	2.77	Involved in tumor cell growth of PCa
mIL-10R	Il10ra	3.12	Cell proliferation, differentiation, and activates transcription factors Stat1 and Stat3
IL-10R2	Il10rb	3.70	Activates JAK proteins
CD132	Il2rg	2.70	Activates JAK proteins
CD124	Il4ra	2.22	Regulates inflammatory, cell-mediated immune response
gp130	Il6st	2.5	Member of Il-6/Stat3 signaling
Jun B	Jun B	2.5	Member of Fos/Jun family, activates AP1 transcription factor
L3	Oas1a	2.22	Involved in immune response
CD140a	Pdgfra	2.70	Receptor that bind and activates JAK proteins, involved in angiogenesis
Cd45	Ptprc	2.77	Receptor that bind and activates JAK proteins
SOCS-1	socs1	2.63	Involved in cell growth
Aprf	Stat3	2.85	Involved in cancer cell survival, inhibition of apoptosis, invasion, and metastasis
No. of genes upregulated in KO mice compared with TG mice			
LL-4	Il4	2.26	Involved in apoptosis
AP-1	Jun	2.83	Cell differentiation
Pr-1	prlr	3.58	Lymphocyte activation

NOTE: Deletion of PKCε in TRAMP mice modulates IL-6/Stat3 signaling–associated genes involved in PCa progression and metastasis. Focused qPCR array for JAK/STAT signaling pathway was carried out in TG and KO PCa as described in Materials and Methods. Table represents the fold increase or decrease in mRNA expression of JAK/STAT signaling–associated genes in KO mice compared with TG mice.

was manifested by significant inhibition of both pStat3Ser727 and pStat3Tyr705 protein levels and decreased Stat3-DNA binding activity. Decrease in Stat3 nuclear staining was observed in PIN and PD adenocarcinoma of KO mice. These results are in accordance with our previously published reports, in which we have shown the interaction of PKCε with Stat3 during development of skin carcinoma in PKCε transgenic mice (24). These data further proves that PKCε may be an initiator for activation of Stat3 during PCa development. IL-6 is involved in activation of Stat3, which phosphorylates tyrosine residue of Stat3. Higher level of serum IL-6 has been associated with larger PCa burden, especially bone metastases (25, 26). In our study, KO mice showed a significant ($P < 0.05$) decrease in serum IL-6 and its receptor gp130, which indicates that PKCε may have a direct or indirect role in potentiating the autocrine loop of IL-6 signaling in PCa. However, further detail investigation is warranted to understand the molecular mechanism of PKCε-mediated IL-6 signaling during the PCa development and metastasis. We further investigated various downstream target genes of Stat3 which have a role in the PCa inflammation, proliferation, angiogenesis, and metastasis (*COX-2, cyclin D1, VEGF, Bcl-xL, IL-6R*) which were significantly inhibited in KO mice. These data further provide evidence that PKCε is linked to activation of Stat3. PCNA is a nuclear

protein, which has been known as a cell proliferative marker, and a decrease in the expression of PCNA reflects cell-cycle arrest in G_1/S phase (27). We observed a significant decrease in the expression of PCNA in KO mice. These data correspond to the previous study, which has shown that knockdown of PKCε in PCa LNCaP cells arrested the cell cycle in G_1/S phase (10). We also conducted focused qRT-PCR arrays of genes involved in the JAK/STAT signaling pathway in TG and KO PCa tissues to determine the role of PKCε in JAK/STAT signaling. A significant decrease in mRNA expression of *CEBPβ, CRP, EGFR, gp130, Jun B*, and *Stat3* was observed in KO mice compared with TG mice (Table 1). These results further provide clues about the role of PKCε in activation of Stat3 and other signaling molecules linked to the PCa development and metastasis. However, a detailed investigation is warranted to find out the cross-talk of PKCε with JAK/STAT signaling pathway–associated molecules.

In summary, deletion of PKCε in FVB/N TRAMP mice inhibits PCa development and metastasis. We have previously reported that Stat3 is a protein partner of PKCε (14, 23). PKCε interacts with Stat3 and phosphorylates Stat3Ser727, essential for Stat3 activation and nuclear localization (14). In consistent with previous findings, deletion of PKCε in FVB/N TRAMP mice downregulated prostatic Stat3 activation and Stat3-regulated gene expressions. We conclude that PKCε and its downstream protein partner Stat3 constitute essential components of the signal transduction pathways involved in PCa development and metastasis. Therefore, we suggest that targeting PKCε is a novel approach for prevention or treatment of PCa.

Disclosure of Potential Conflicts of Interest

No potential conflicts of interest were disclosed.

Grant Support

This study was supported by DOD grant (W81XWH), NIH grant CA35368, and UWCCC Cancer Center Support grant 2 P30 CA014520-34 for small animal imaging facility.

The costs of publication of this article were defrayed in part by the payment of page charges. This article must therefore be hereby marked advertisement in accordance with 18 U.S.C. Section 1734 solely to indicate this fact.

Received November 17, 2010; revised January 21, 2011; accepted January 26, 2011; published online March 15, 2011.

References

1. Jemal A, Siegel R, Xu J, Ward E. Cancer statistics. CA Cancer J Clin 2010;60:277–300.
2. Cooperberg MR, Broering JM, Carroll PR. Risk assessment for prostate cancer metastasis and mortality at the time of diagnosis. J Natl Cancer Inst 2009;16101:878–87.
3. Nishizuka Y. The protein kinase C family and lipid mediators for transmembrane signaling and cell regulation. Alcohol Clin Exp Res 2001;25Suppl ISBRA:3S–7S.
4. Newton AC. Protein kinase C: structural and spatial regulation by phosphorylation, cofactors, and macromolecular interactions. Chem Rev 2001;101:2353–64.
5. Mellor H, Parker PJ. The extended protein kinase C superfamily. Biochem J 1998;332:281–92.
6. Kazanietz MG. Eyes wide shut: protein kinase C isozymes are not the only receptors for the phorbol ester tumor promoters. Mol Carcinog 2000;28:5–11.
7. Denning MF. Epidermal keratinocytes: regulation of multiple cell phenotypes by multiple protein kinase C isoforms. Int J Biochem Cell Biol 2004;36:1141–6.
8. Cacace AM, Guadagno SN, Krauss RS, Fabbro D, Weinstein IB. The epsilon isoform of protein kinase C is an oncogene when overexpressed in rat fibroblasts. Oncogene 1993;8:2095–104.
9. Kazanietz MG, editor. Protein Kinase C in Cancer Signaling and Therapy. New York: Springer; 2010.
10. Wu D, Foreman TL, Gregory CW. Protein kinase C epsilon has the potential to advance the recurrence of human prostate cancer. Cancer Res 2002;62:2423–9.
11. Meshki J, Caino MC, von Burstin VA, Griner E, Kazanietz MG. Regulation of prostate cancer cell survival by protein kinase Cepsilon involves bad phosphorylation and modulation of the TNFalpha/JNK pathway. J Biol Chem 2010;285:26033–40.
12. Wu D, Thakore CU, Wescott GG, McCubrey JA, Terrian DM. Integrin signaling links protein kinase Cepsilon to the protein kinase B/Akt survival pathway in recurrent prostate cancer cells. Oncogene 2004;23:8659–72.
13. McJilton MA, Van Sikes C, Wescott GG. Protein kinase Cepsilon interacts with Bax and promotes survival of human prostate cancer cells. Oncogene 2003;22:7958–68.
14. Aziz MH, Manoharan HT, Church DR, Dreckschmidt NE, Zhong W, Oberley TD, et al. Protein kinase C epsilon interacts with signal transducers and activators of transcription 3 (Stat3), phosphorylates Stat3Ser727, and regulates its constitutive activation in prostate cancer. Cancer Res 2007;67:8828–38.
15. Aziz MH, Dreckschmidt NE, Verma AK. Plumbagin, a medicinal plant-derived naphthoquinone, is a novel inhibitor of the growth and invasion of hormone-refractory prostate cancer. Cancer Res 2008;68:9024–32.
16. Pinchuk AN, Rampy MA, Longino MA, Skinner RW, Gross MD, Weichert JP, et al. Synthesis and structure activity relationship effects on the tumor avidity of radioiodinated phospholipid ether analogs. J Med Chem 2006;49:2155–65.
17. Abdulghani J, Gu L, Dagvadorj A, Lutz J, Leiby B, Bonuccelli G, et al. Stat3 promotes metastatic progression of prostate cancer. Am J Pathol 2008;172:1717–28.
18. Chan KS, Sano S, Kiguchi K, Anders J, Komazawa N, Takeda J, et al. Disruption of Stat3 reveals a critical role in both the initiation and the promotion stages of epithelial carcinogenesis. J Clin Invest 2004;114:720–28.
19. Alvarez JV, Febbo PG, Ramaswamy S, Loda M, Richardson A, Frank DA. Identification of a genetic signature of activated signal transducer and activator of transcription 3 in human tumors. Cancer Res 2005;65:5054–62.
20. Huang HF, Murphy TF, Shu P, Barton AB, Barton BE. Stable expression of constitutively-activated STAT3 in benign prostatic epithelial cells changes their phenotype to that resembling malignant cells. Mol Cancer 2005;12:4–12.
21. Shukla S, MacLennan GT, Marengo SR, Resnick NI, Gupta S. Constitutive activation of PI3K-Akt and NF-kappa B during prostate cancer progression in autochthonous transgenic mouse model. Prostate 2005;64:224–39.
22. Greenberg NM, DeMayo F, Finegold MJ, Medina D, Tilley WD, Aspinall JO, et al. Prostate cancer in a transgenic mouse. Proc Natl Acad Sci U S A 1995;92:3439–43.
23. Aziz MH, Hafeez BB, Sand JM, Pierce DB, Aziz SW, Dreckschmidt NE, et al. Protein kinase C epsilon mediates Stat3Ser727 phosphorylation, Stat3-regulated gene expression, and cell invasion in various human

cancer cell lines through integration with MAPK cascade (RAF-1, MEK1/2, and ERK1/2). Oncogene 2010;29:3100–9.
24. Aziz MH, Manoharan HT, Sand JM, Verma AK. Protein kinase Cepsilon interacts with Stat3 and regulates its activation that is essential for the development of skin cancer. Mol Carcinog 2007;46:646–53.
25. Drachenberg DE, Elgamal AA, Rowbotham R, Peterson M, Murphy GP. Circulating levels of IL-6 in patients with hormone refractory prostate cancer. Prostate 1999;41:127–33.
26. Adler HL, McCurdy MA, Kattan MW, Timme TL, Scardino PT, Thompson TC. Elevated levels of circulating interleukin-6 and transforming growth factor-beta1 in patients with metastatic prostatic carcinoma. J Urol 1999;161:182–7.
27. Zhong W, Peng J, He H, Wu D, Han Z, Bi X, et al. Ki-67 and PCNA expression in prostate cancer and benign prostatic hyperplasia. Clin Invest Med 2008;31:8–15.